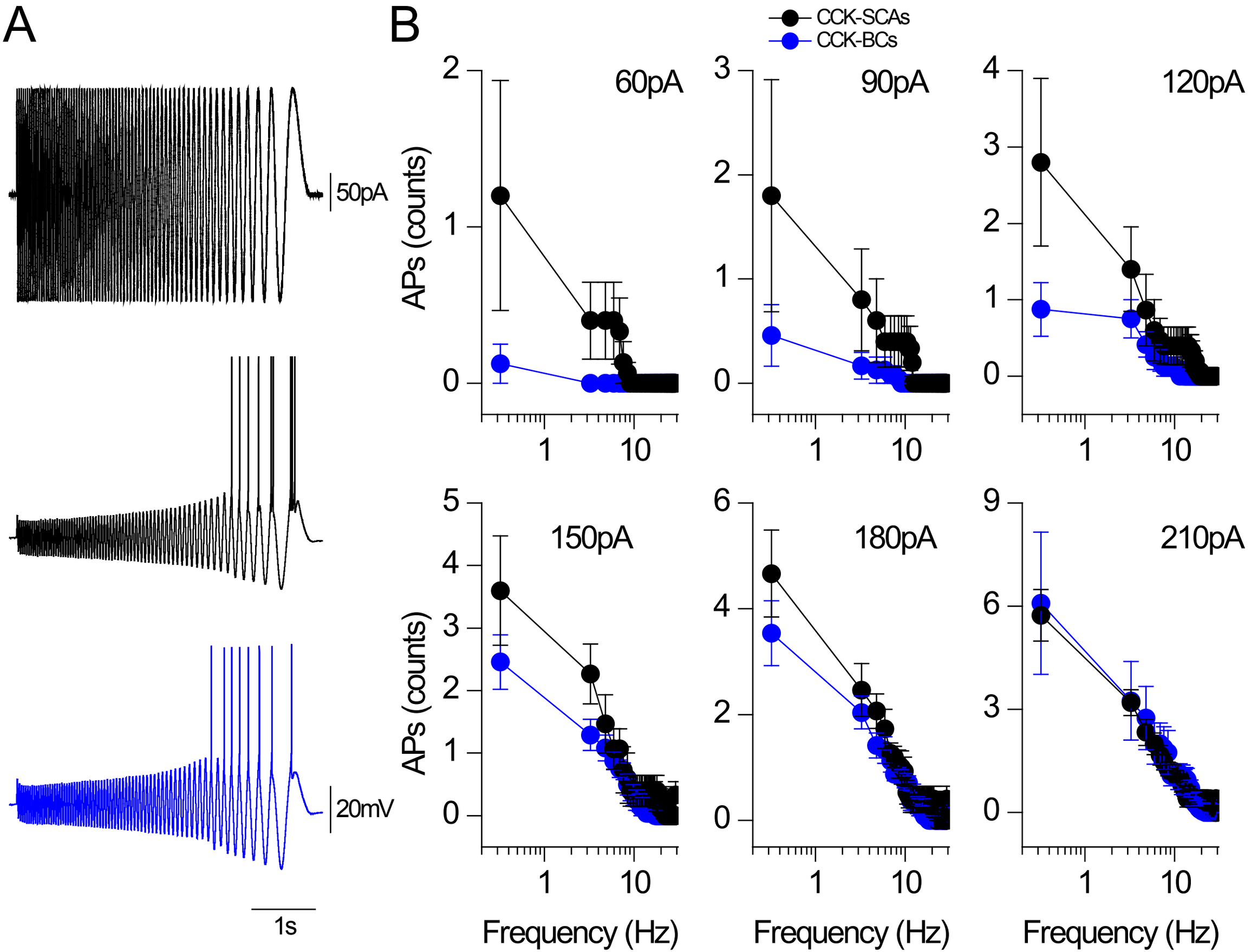

Fig S1. SCAs and BCs display similar firing activity engagement properties to different sinusoidal inputs. (A) Representative 150pA “zap” sinusoidal current injection (30-1Hz left to right), and representative response traces for CCK-SCAs (black) and CCK-BCs (blue). (B) Spike output activity of CCK-SCAs (black) and CCK-BCs (blue) in response to sinusoidal zap current injections ranging in amplitude from 60 to 210pA delivered at frequencies between 1 to 30Hz.

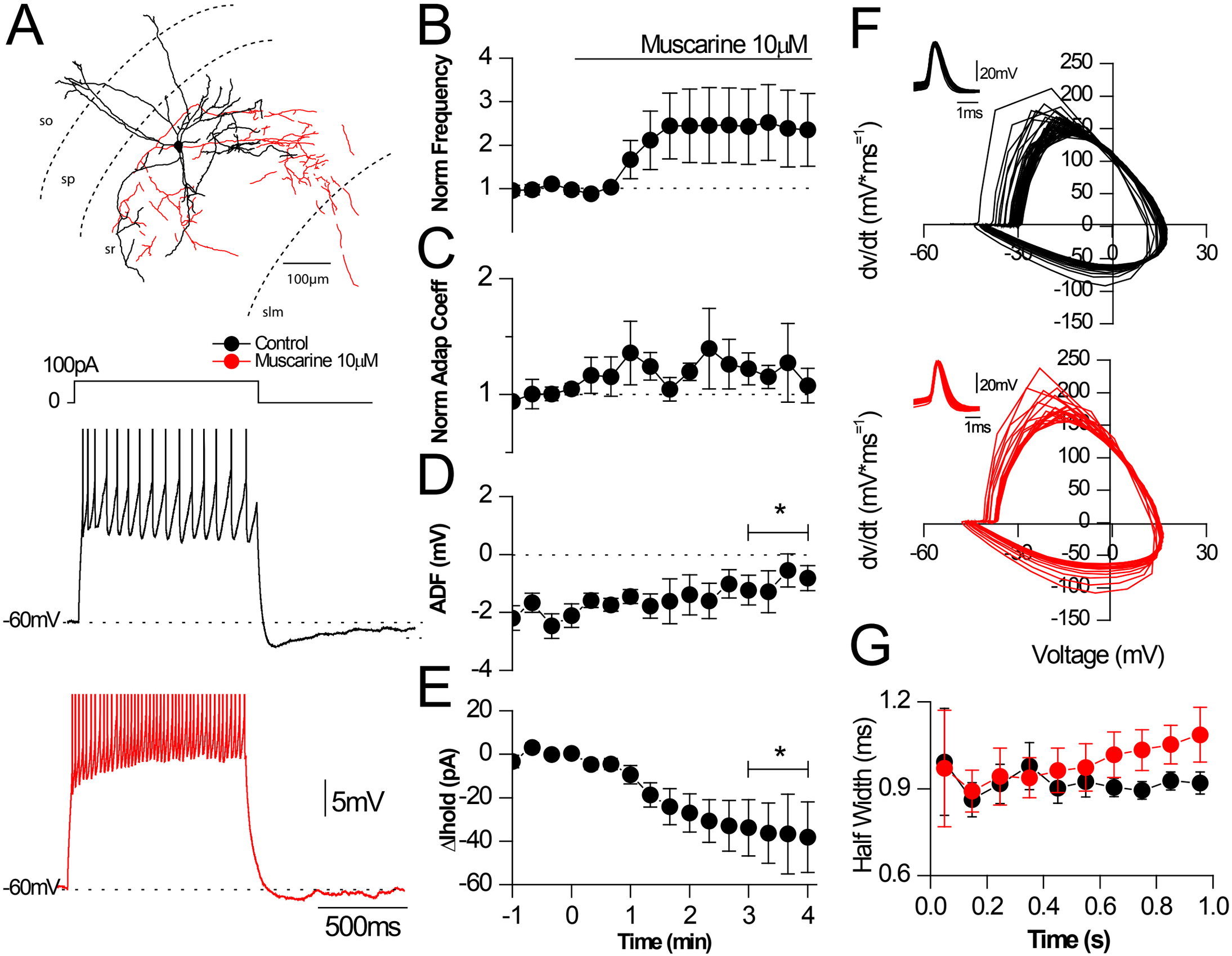

Fig S2. Cholinergic modulation of CCK-lacking radiatum projecting cells (A) Camera Lucida drawing of representative CCK-lacking radiatum projecting cell and representative voltage response to a 100pA electrotonic current pulse (1sec duration) from -60 mV in (black) control and (red) after bath application of 10 µM muscarine. (B) Time course of AP frequency changes in response to muscarine normalized to the first min. (C) Adaptation coefficient normalized to the first min. (D) Afterdeflection (ADF) observed in a 200 ms window after the electrotonic current pulse offset (E) The time course of change in holding current in the presence of muscarinic receptor activation. (F) Representative phase plots of dV/dt vs. voltage of APs for CCK-lacking radiatum projecting cells in (black) control conditions and (red) after bath application of 10µM muscarine and (G) AP half-width, binned in 100 ms intervals during the 1 sec current step for a population of 5 CCK-lacking radiatum projecting cells in (black) control conditions and (red) after bath application of 10µM muscarine.

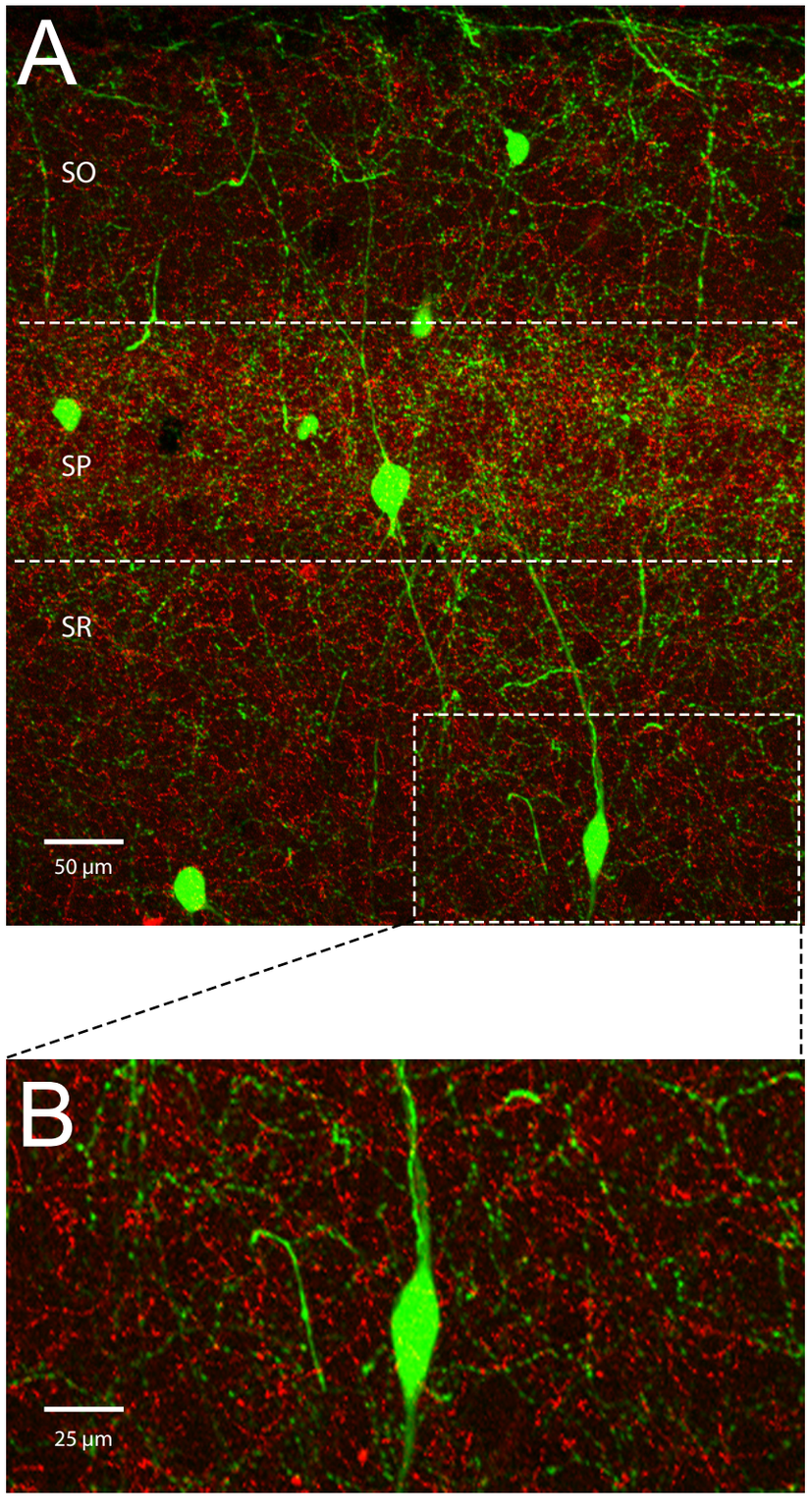

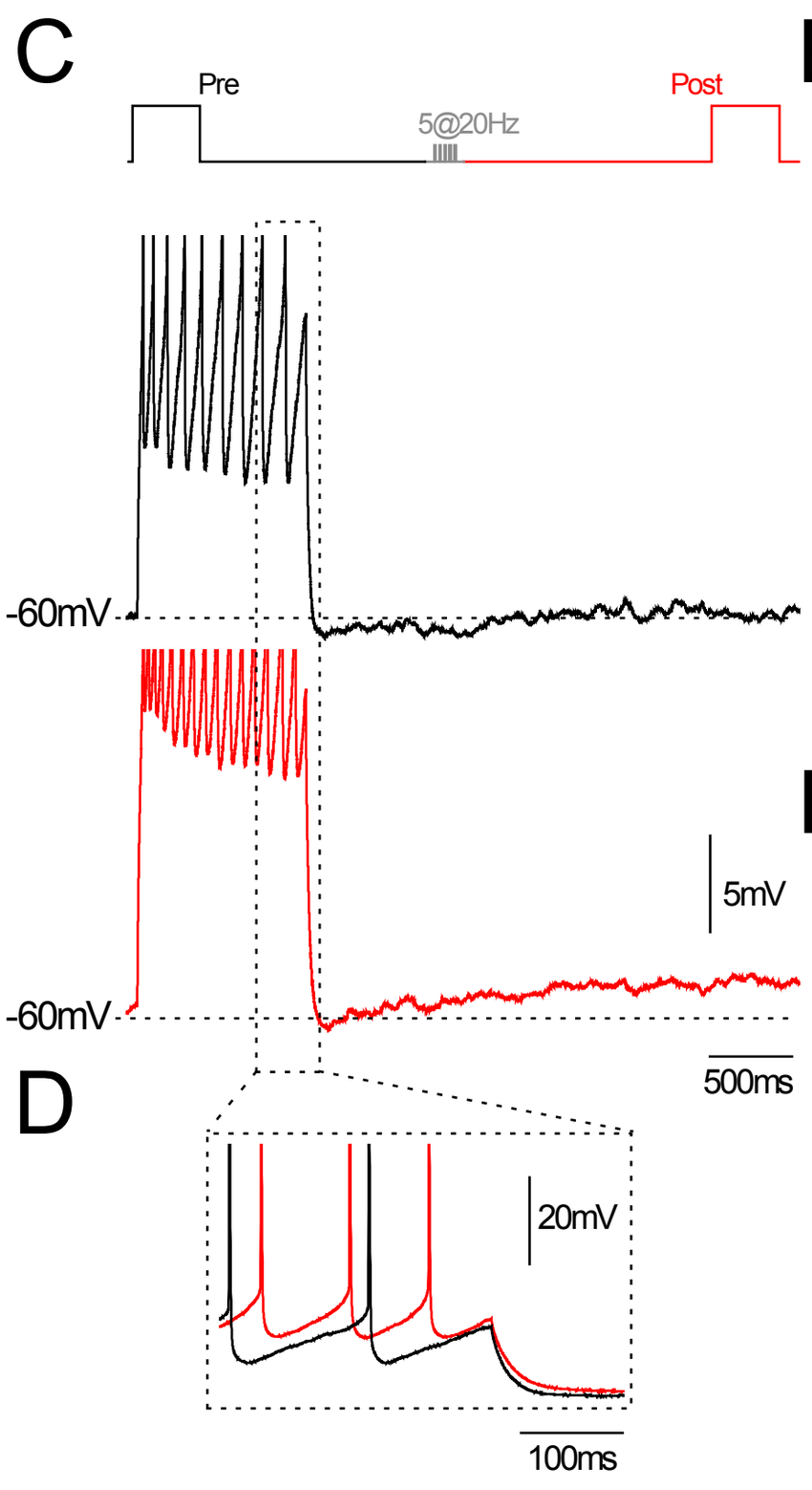

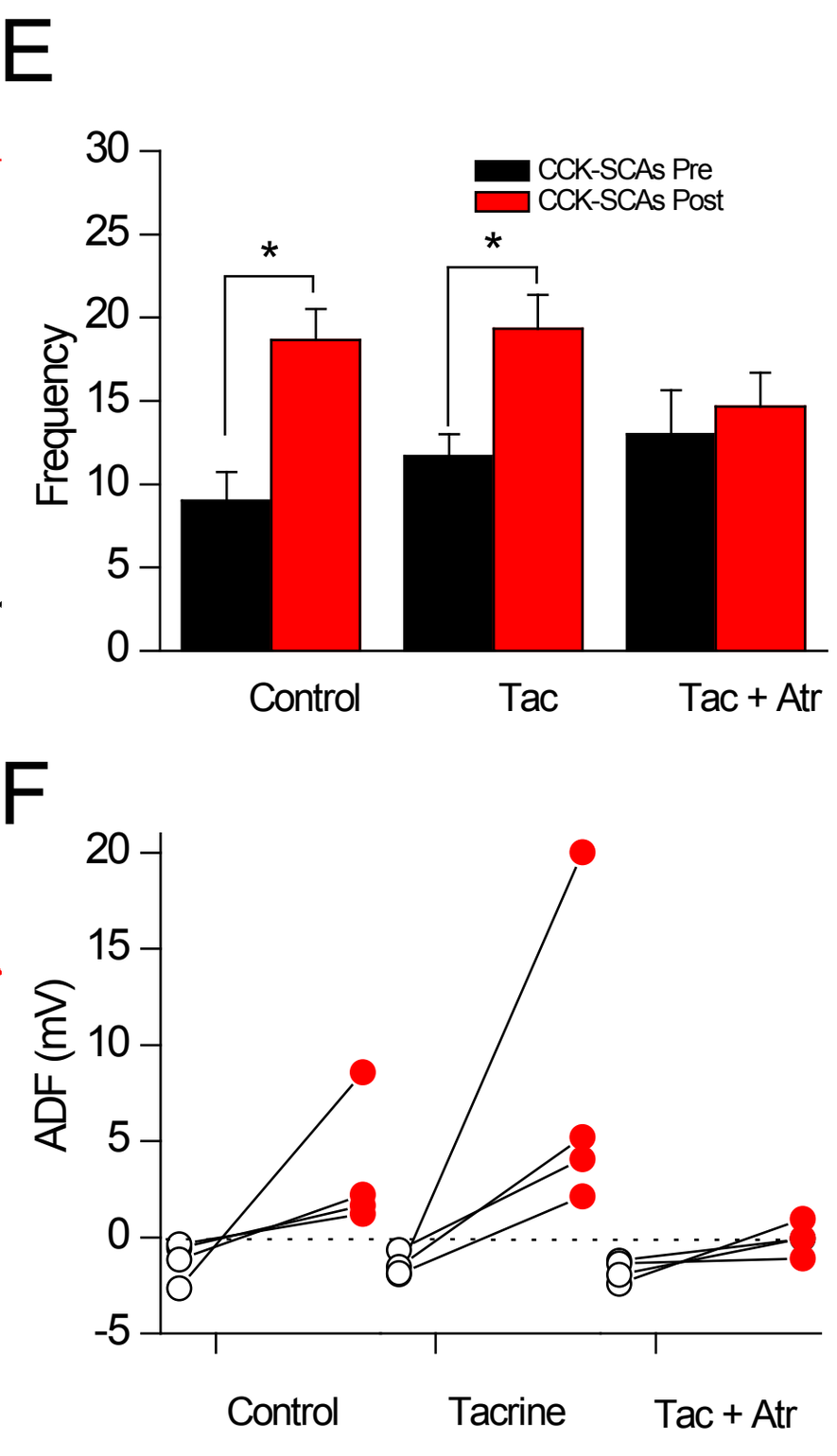

Fig S3. Endogenous acetylcholine release triggers an increase in action potential firing frequency and a gain of ADP in CCK-SCAs. (A) Images of 2D flat projections of three-dimensional confocal image stacks of vAChT-immunoreactive terminal labeling (red) in the vicinity of CA1 GAD65-GFP cells (green) (B) Same image as seen in (A) but limited to an interneuron located in stratum radiatum (C) Schematic representation of cholinergic fiber stimulation protocol and representative traces pre (black) and post (red) fiber stimulations. (D) Inset shows the increase in firing activity elicited by ACh release (E) Summary plot of the action potential firing frequency ratio (poststimulation/prestimulation) in control, in the presence of the cholinesterase inhibitor, tacrine (20µM) and in the presence of tacrine plus the muscarinic receptor antagonist atropine (5µM). (F) Summary plot of the ADF for individual cells before and after stimulation in CCK-SCAs.

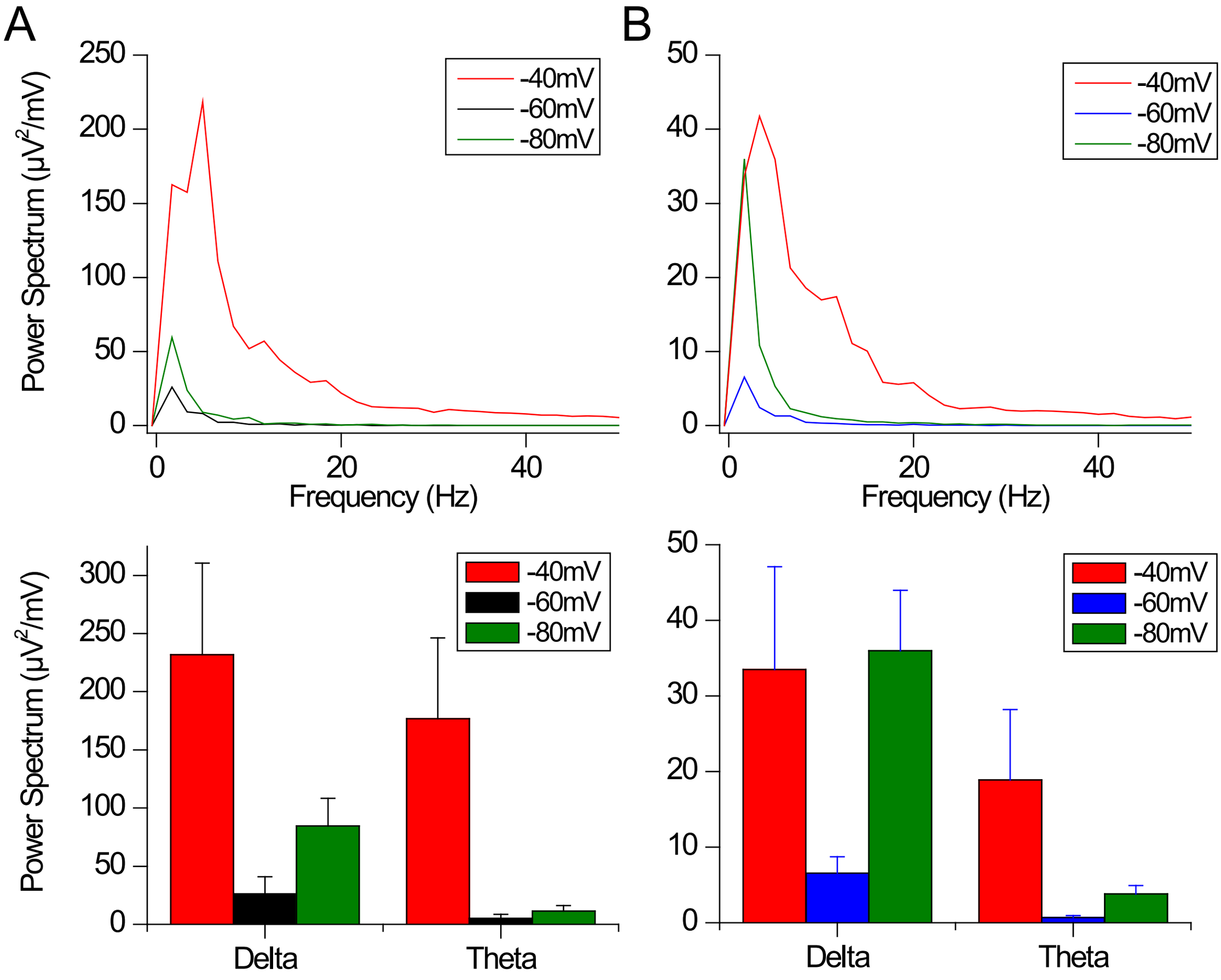

Fig S4. Relationship between membrane holding potential and MPOs. (A) Power spectrum plots and quantification bar plot for delta (1-2 Hz) and theta frequency (4-8 Hz) ranges at -40, -60 and -80mV membrane holding potentials in CCK-SCAs. (B) Power spectrum plot and quantification bar plot for delta and theta frequency ranges at -40, -60 and -80mV membrane holding potentials in CCK-BCs

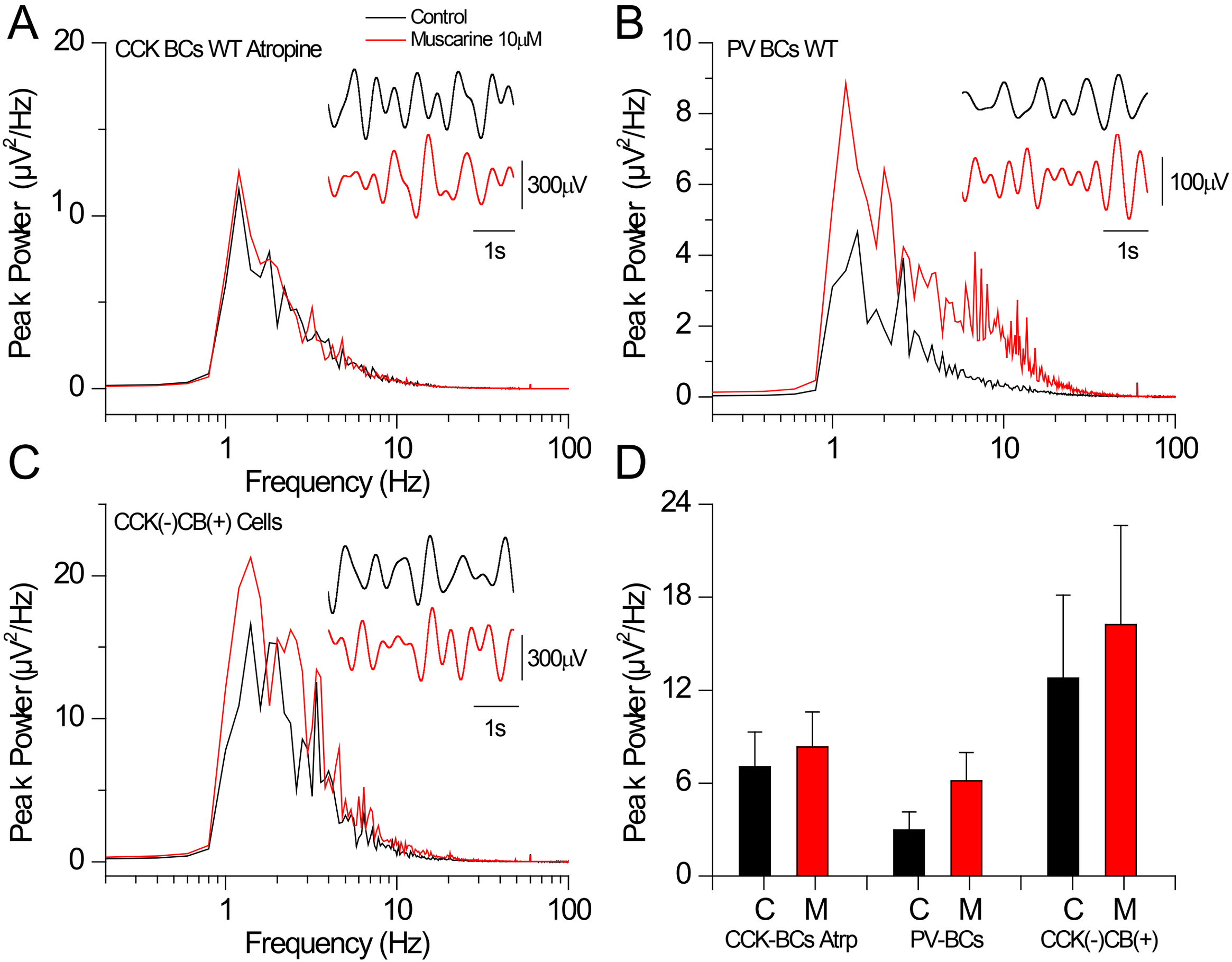

Fig S5. Power spectrum plot of subtreshold activity (holding Vm at -60mV) for (A) CCK-BCs WT in response to muscarine in the presence of atropine 50μM, (B) PV-BCs WT, and (C) CCK-lacking radiatum projecting cell populations data in control conditions (black trace) and muscarine 10μM (red trace). The insets show 5 seconds holding resting potential raw traces filtered between 0.8 to 2.2Hz (MPOs peak power for CCK-SCAs and CCK-BCs) in control (black) and muscarine (red) conditions. (D) Bar plot of the population average MPOs peak data between 1 to 2Hz for each condition.